Homopolar bonds in Se-rich Ge–As–Se chalcogenide glasses*

Si-Wei Xu(许思维)[1,2], Rong-Ping Wang(王荣平)[2,†], Zhi-Yong Yang(杨志勇)[3], Li Wang(王丽)[1], and Luther-Davies Barry[2]

[1] College of Applied Sciences, Beijing University of Technology, Beijing 100124, China
[2] Laser Physics Centre, Research School of Physical Science and Engineering, Australian National University, Canberra, ACT 0200, Australia
[3] College of Physics and Electronic Engineering, Jiangsu Normal University, Xuzhou 221116, China

(Received 2 December 2015; revised manuscript received 6 January 2016; published online 1 April 2016)

We have prepared three groups of Ge–As–Se glasses in which the Se content is 5.5 mol%, 10 mol%, and 20 mol% rich, respectively. We explored the possibility of suppressing the formation of the Ge–Ge and As–As homopolar bonds in the glasses. Thermal kinetics analysis indicated that the 5.5 mol% Se-rich $Ge_{11.5}As_{24}Se_{64.5}$ glass exhibits the minimum fragility and thus is most stable against structural relaxation. Analysis of the Raman spectra of the glasses indicated that the Ge–Ge and As–As homopolar bonds could be almost completely suppressed in 20 mol% Se-rich $Ge_{15}As_{14}Se_{71}$ glass.

Keywords: chalcogenide glasses, structure, differential scanning calorimetry, Raman scattering

PACS: 71.23.Cq, 79.60.Ht, 81.70.Pg, 33.20.Fb **DOI:** 10.1088/1674-1056/25/5/057105

1. Introduction

Chalcogenides are materials containing one of the chalcogen elements (S, Se, and Te) covalently bonded to the elements such as Ge, As, Si, and Sb. Depending on their chemical composition and structure, chalcogenides can display metallic, semi-conducting, or insulating properties. They have an increasing number of important applications in electronics and photonics because of their high optical nonlinearity and wide transmission range.[1–5] For example, researchers have used chalcogenide glasses for all-optical processing of high speed telecommunication signals.[6,7] It has been demonstrated that the glass properties can be tuned in a widely compositional range, therefore, it is possible to optimize the glasses for specific applications by tuning the material composition.[8–10]

Low optical loss and high stability are two important parameters for the application of the glasses in photonics. In terms of stability, Bulla *et al.* and Su *et al.* investigated the properties of Ge–As–Se thin films with different chemical compositions,[11,12] and found that stable glass films exist for a mean coordination number (MCN) of 2.45, where MCN is the sum of the products of the individual abundance times the coordination of the constituent atoms.[13] More recently, Ting *et al.* investigated 34 samples of Ge–As–Se glasses with compositions distributed across the glass forming region and covering wide ranges of stoichiometry and MCN. In these samples, the activation energy for enthalpy relaxation showed a sharp minimum at the percolation threshold MCN = 2.40, but the minimum extended to cover a wide range of non-stoichiometric glasses which were up to 20 mol% Se-rich.[9] On the other hand, the fragility, which is defined by the rate at which the constraints are broken with increasing temperature above T_g, appears to be rather independent of MCN but is controlled by the departure from stoichiometry. Therefore, MCN is considered only properly defined at low temperature.[9] The activation energy at T_g may correlate with MCN because it reflects the energy required to gain mobility relative to a state where all constraints are intact. Therefore, strong glasses with the smallest fragility indices are relatively stable against structure relaxation and are likely to be the best for the applications in photonics.

In terms of optical loss, our evidence indicates that the losses in the glasses are correlated with the number of the Ge–Ge and As–As homopolar bonds.[14,15] Ideally, such homopolar bonds should be completely suppressed in chemically stoichiometric glasses since all chalcogen elements should be consumed by the network-forming elements such as Ge, As, and Sb. However, it has been found that homopolar Ge–Ge, As–As, and Sb–Sb bonds all exist in chalcogen-rich glasses and chalcogen–chalcogen bonds even exist in chalcogen-poor glasses.[16,17] Our recent measurements of Raman and x-ray photoelectron spectra confirmed that finite numbers of homopolar Ge–Ge and As–As bonds appeared, indicating that Se was not always bonded with Ge or As in chemically stoichiometric Ge–As–Se glasses.[18] It is expected that, increasing the Se concentration can eliminate the Ge–Ge and As–As homopolar bonds in the Se-rich glasses. Moreover, it is possible to identify the Se-rich glasses that have the minimum fragility index with stable properties against structural relaxation.

To elucidate this, we prepared three groups of Se-rich Ge–As–Se glasses (5.5 mol%, 10 mol%, and 20 mol% Se-rich, re-

*Project supported by the Australian Research Council (ARC) Centre of Excellence for Ultrahigh Bandwidth Device for Optical System (Project CE110001018), Australian Research Council Discovery Programs (Project DP110102753), and the Importation and Development of High-Caliber Talents Project of Beijing Municipal Institutions, China.

†Corresponding author. E-mail: rpw111@rsphysse.anu.edu.au

© 2016 Chinese Physical Society and IOP Publishing Ltd

spectively). We measured the Raman scattering spectra of the glasses, and decomposed them into different structural units with the aim of understanding the evolution of the number of homopolar bonds as a function of the chemical composition.

2. Experiment

$Ge_xAs_ySe_{1-x-y}$ bulk glasses were prepared by the melt-quenching technique. High purity (5N) raw materials Ge, As, and Se were weighed (15 g) inside a dry nitrogen glove box and loaded into a pre-cleaned quartz ampoule, which was then evacuated to 10^{-6} Torr and dried at 160 °C for 4 h to ensure the removal of surface moisture from the raw materials. The ampoule was sealed under a vacuum using an oxygen hydrogen torch, and introduced into a rocking furnace to melt the contents at 900 °C for 30 h. Then the ampoule was removed from the rocking furnace and quenched in air. Subsequently, the glass sample was annealed below the glass transition temperature T_g and finally slowly cooled to room temperature.

The quality of the glasses was examined using x-ray diffraction (XRD) and infrared (IR) microscopy. The XRD patterns indicated that the glass structure was amorphous, and the IR microscopy revealed the absence of any observable bubbles in all the samples. The x-ray energy dispersive spectra (EDS) were used to check the composition of the glasses. Generally, we examined several different positions. We found that the fluctuations in the glass compositions were less than 0.5%. The glass transition temperatures (T_g) were measured using a differential scanning calorimetry (DSC) (Mettler-Toledo, DSC1) with different scanning rates from 5 K/min to 30 K/min under a uniform nitrogen gas flow of 50 mL/min. In all cases, we raised the temperature above T_g to erase the thermal history in the first run, and then the inflection point along the step transition in the second run was read as T_g using STARe analysis software (Mettler-Toledo) and the error bar of the reading was within 0.5 °C. The activation energy and fragility were extracted from T_g measurements using the procedure presented in Ref. [9].

Raman spectra were recorded using a T64000 Jobin-Yvon-Horiba micro-Raman spectrometer equipped with a liquid-nitrogen-cooled CCD detector. The 830 nm laser line was used as an excitation source, and the laser power was kept as small as possible to avoid any photo-induced effects. The resolution of the spectrometer was about 0.5 cm^{-1}. We first collected Raman spectra from various parts of the glass rod. The identical profiles of the spectra indicated the homogenization of the glass. Then the Raman spectra were reduced by the removal of the Bose–Einstein factors following the standard procedures and then were decomposed into different structural units.[18] We used PeakFit software and an iterative method to simulate the peak center, full width at half maximum, and the height of each Raman vibrational peak. In all cases, we only set up the initial value of the peak position, the final value of the real position could be different. In other words, the individual Raman peak had the freedom to change its position, width, and height during the fitting process.

3. Results and discussion

It is well accepted that T_g is a measure of the glass network connectivity. All the compositions we studied are in the glass-forming region and have an MCN between 2.4 and 2.6, and therefore should have a continuous network structure.[19,20] Therefore, with increasing content of 4-folded coordinated Ge, the MCN increases and the glass exhibits better network connectivity which corresponds to an increasing T_g. This is evident as shown in the fourth column of Table 1, where T_g almost linearly increases as a function of MCN. The activation energy and the fragility index of the glasses are shown in the fifth and the last columns of Table 1, respectively. The activity energy increases with increasing MCN, while the fragility index exhibits a minimum for each group of glasses.

Table 1. Composition and corresponding mean coordination number (MCN), glass transition temperature (T_g), activation energy (E_a), and fragility index (m) of $Ge_xAs_ySe_{1-x-y}$ glasses.

Composition	MCN	Se-rich/mol%	T_g/°C	E_a/eV	m
$Ge_{5.5}As_{31.2}Se_{63.3}$	2.442	5.5	176.9±0.1	2.40	26.92
$Ge_{8.5}As_{27.6}Se_{63.9}$	2.446	5.5	189.3±0.3	2.42	26.36
$Ge_{11.5}As_{24}Se_{64.5}$	2.47	5.5	200.6±0.3	2.44	26.03
$Ge_{14.5}As_{20.4}Se_{65.1}$	2.494	5.5	217.1±0.3	2.54	26.13
$Ge_{17.5}As_{16.8}Se_{65.7}$	2.518	5.5	230.8±0.3	2.62	26.27
$Ge_5As_{30}Se_{65}$	2.40	10	165.2±0.2	2.42	27.88
$Ge_{10}As_{24}Se_{66}$	2.44	10	182.0±0.1	2.46	27.28
$Ge_{15}As_{18}Se_{67}$	2.48	10	201.5±0.1	2.55	27.12
$Ge_{20}As_{12}Se_{68}$	2.52	10	224.5±0.2	2.70	27.34
$Ge_{25}As_6Se_{69}$	2.56	10	245.4±0.2	2.95	28.74
$Ge_{10}As_{20}Se_{70}$	2.40	20	156.1±0.3	2.48	29.12
$Ge_{12.5}As_{17}Se_{70.5}$	2.42	20	167.3±0.2	2.49	28.57
$Ge_{15}As_{14}Se_{71}$	2.44	20	178.5±0.1	2.51	27.99
$Ge_{17.5}As_{11}Se_{71.5}$	2.46	20	185.9±0.2	2.56	28.12
$Ge_{22.5}As_5Se_{72.5}$	2.50	20	210.4±0.3	2.72	28.34

The compositions and the corresponding MCN, T_g, E_a, and m of $Ge_xAs_ySe_{1-x-y}$ glasses are reported in Table 1. The results indicate that T_g increases with increasing MCN but the glass transition activation energy exhibits a minimum at around MCN = 2.4. Since the MCNs of all our glasses are larger than 2.4, the trends are in excellent agreement with the results in Ref. [9]. On the other hand, it is found that the fluctuation of fragility is less than 1.2 for the glasses with the same level of additional Se, whilst the difference between 5.5 mol% and 20 mol% Se-rich glasses is ∼2, indicating that the fragility appears to be rather independent of MCN but is controlled by the departure from stoichiometry.

Indeed, the fragility defines the rate at which the system departs from equilibrium upon losing ergodicity, thus it reflects the tendency of the glass to undergo structural relaxation below T_g. Chalcogenide glasses usually have low T_g and thus the relaxation processes could be significant even at room temperature. A fragile glassy system departs from equilibrium at a faster rate than a strong system, and this is highly undesirable for applications such as integrated infrared optics where the relaxation processes can lead to the change of the physical properties like refractive index and bandgap which may degrade the device performance.[11,12,14,21] The last column in Table 1 suggests that 5.5 mol% Se-rich $Ge_{11.5}As_{24}Se_{64.5}$ with an MCN of 2.47 could be the most stable glass.

Raman spectra of the glasses are recorded from 150 cm^{-1} to 350 cm^{-1}. Generally, there are two broad bands. One is centered at 200 cm^{-1} and the other is at 230 cm^{-1} with a broad tail extending to 300 cm^{-1}. It is well accepted that depending on the composition, $GeSe_{4/2}$ tetrahedral $AsSe_{3/2}$ pyramidal, and some homopolar bonds are cross-linked to form the Ge–As–Se glass network. Corner-sharing (CS) and edge-sharing (ES) $GeSe_{4/2}$ tetrahedral units have Raman peaks at 195 cm^{-1} and 213 cm^{-1}, respectively.[22,23] $AsSe_{3/2}$ pyramidal units have Raman peaks at 230 cm^{-1} and 268 cm^{-1}.[18] The peak at 250 cm^{-1} is due to the vibrational modes of Se chains or rings.[22] One peak at 175 cm^{-1} and another peak at 300 cm^{-1} are the characteristic of the Ge–Ge mode of the ethane-like (Se3)Ge–Ge(Se3) structural unit.[24,25] The peak at 247 cm^{-1} is ascribed to the As–As vibration modes.[18,26–30]

In order to quantify the structural evolution, the Raman spectra of these glasses (5.5 mol%, 10 mol%, and 20 mol% Se-rich, respectively) are decomposed into multiple Gaussians based on the structural units. Figure 1 shows the results of the decomposition of the Raman spectra of the 5.5 mol% Se-rich glasses. The corner-sharing $GeSe_{4/2}$ and edge-sharing $GeSe_{4/2}$ appear at around 198 cm^{-1} and 213 cm^{-1}, respectively. Their intensities increase with increasing Ge concentration. In contrast, the intensities of the peaks at 247 cm^{-1} and 268 cm^{-1} decrease with decreasing As concentration, and the positions of these two peaks slightly shift toward a lower wavenumber with increasing Ge concentration. Only a small number of homopolar Se–Se bonds exist. Moreover, weak vibrations of the homopolar Ge–Ge bonds appear in the glasses containing a high concentration of Ge. The peak at 300 cm^{-1} due to the Ge–Ge vibrations appears in $Ge_{14.5}As_{20.4}Se_{65.1}$ glasses and its intensity increases with increasing Ge concentration.

Figures 2(a) and 2(b) show the decomposition of the Raman spectra of the 10 mol% and 20 mol% Se-rich glasses, respectively. The results are basically consistent with those in Fig. 1. We observe that the homopolar Ge–Ge and As–As vibrations seem to appear only when the Ge or As concentration is high, for example, Ge–Ge homopolar vibrations appear in the samples containing more than 20 mol% Ge (Fig. 2(a)) and more than 17.5 mol% Ge (Fig. 2(b)), while As–As homopolar vibrations appear in the samples with more than 18 mol% As (Fig. 2(a)) and more than 17 mol% As (Fig. 2(b)). In all cases, homopolar Se–Se bonds cannot be completely suppressed.

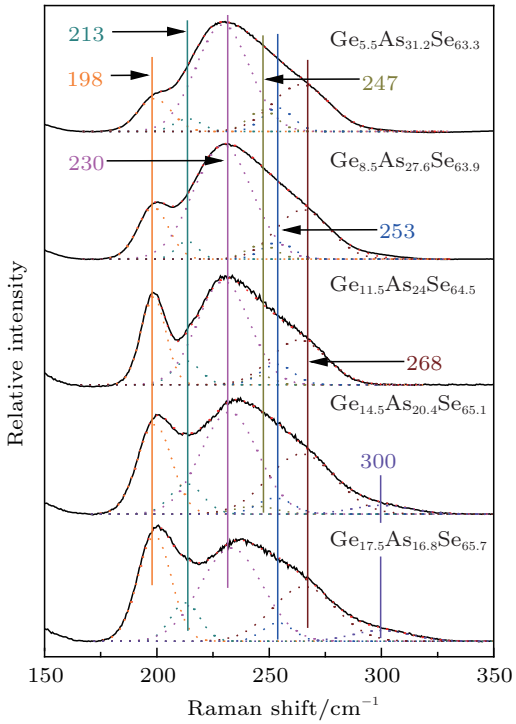


Fig. 1. (color online) Raman spectra of the 5.5 mol% Se-rich glasses with different chemical compositions and their decompositions.

The relative ratio of the integrated area of each decomposed peak to that of the whole area of Raman spectra as a function of MCN is plotted in Fig. 3. The contribution of Ge–Se increases while that of As–Se decreases with increasing MCN. Special care is taken to the distribution of homopolar Ge–Ge, As–As, and Se–Se bonds. In order to clearly see the evolution of the bonds, we plot the relative ratios of these bonds on the same scale, e.g., from 0 to 15% in the vertical axis. Obviously, Se–Se bonds exist in all cases and the content changes from 3% up to about 11% for the most Se-rich compositions. On the other hand, Ge–Ge bonds can be suppressed in the glasses with low MCN and As–As bonds disappear at high MCN. The sum of the Ge–Ge and As–As homopolar bonds (Fig. 4) exhibits a minimum at MCN near 2.45.

For the evolution of the chemical bonds in Fig. 3, we are most interested in the evolution of the numbers of the homopolar Ge–Ge and As–As bonds. Because all the glasses are Se-rich, Se–Se bonds should appear in all cases, but these bonds do not appear to seriously contribute to the optical losses of the glasses.[15] In one of our previous papers, we have shown that it appears to be impossible to completely

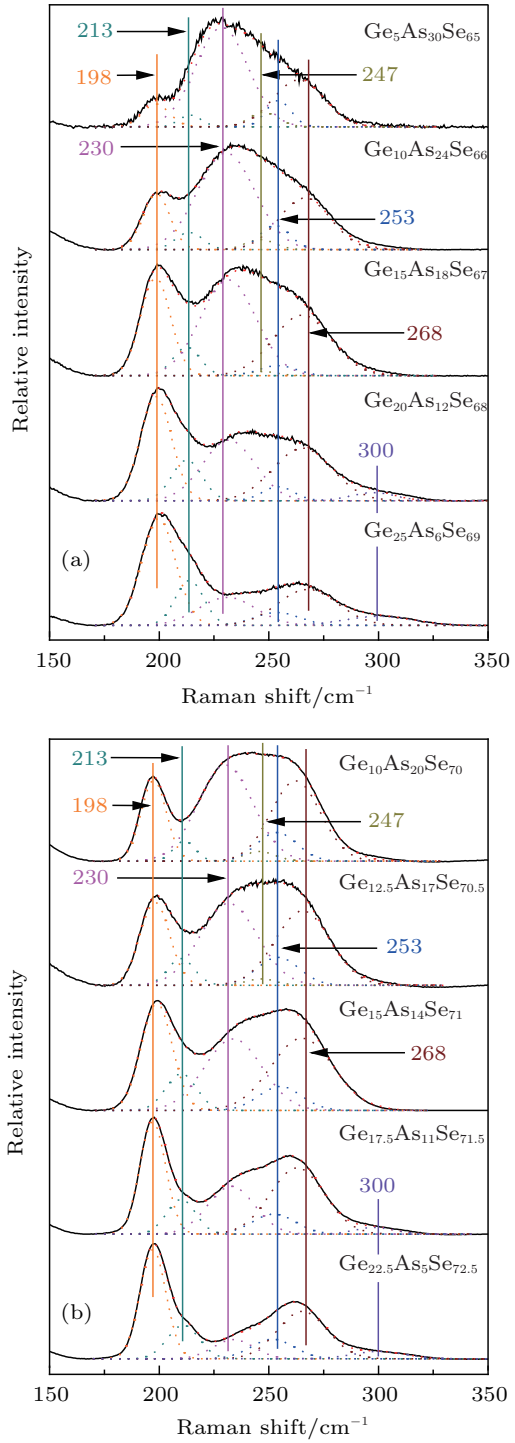


Fig. 2. (color online) (a) Raman spectra of the 10 mol% Se-rich glasses with different chemical compositions and their decompositions. (b) Raman spectra of the 20 mol% Se-rich glasses with different chemical compositions and their decompositions.

suppress both Ge–Ge and As–As bonds in chemically stoichiometric glasses.[18] One might expect that the residual Ge and As should be bonded with Se if the Se content in the glass is further increased. By plotting the total number of Ge–Ge and As–As bonds as a function of MCN (Fig. 4), it becomes evident that the Ge–Ge and As–As homopolar bonds can be completely suppressed in the 20 mol% Se-rich $Ge_{15}As_{14}Se_{71}$ glass. Since it appears that the optical losses in the glasses are primarily determined by the exponential absorption tail associated with the Ge–Ge and As–As homopolar bonds,[15] the present results imply that Se-rich glasses such as $Ge_{15}As_{14}Se_{71}$ should be the best for the applications such as optical fibers, as the interaction pathway in fiber is long and enhanced optical losses could significantly degrade the performance of fiber devices.

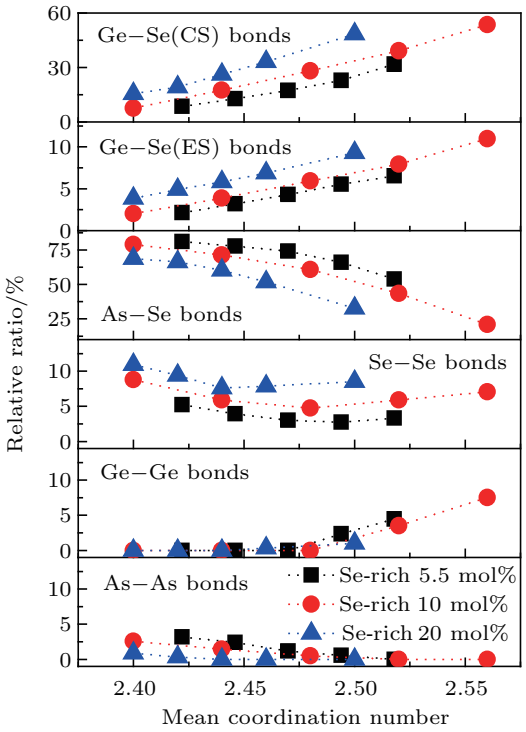


Fig. 3. (color online) Relative number of the chemical bonds derived from the simulation of each Raman spectrum according to the area under each fitted peak in ratio to the total area under the spectrum.

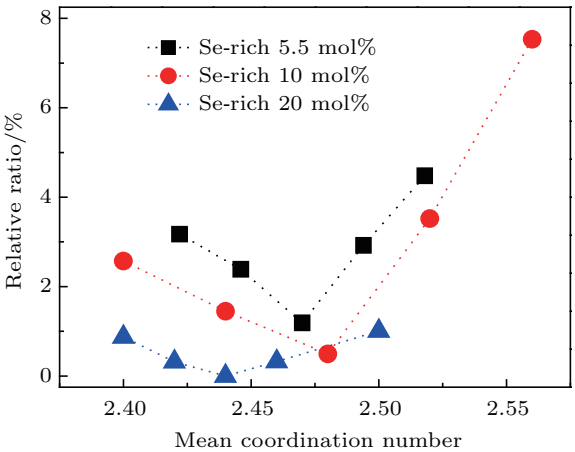


Fig. 4. (color online) Total number of Ge–Ge and As–As homopolar bonds as a function of MCN derived from the sum of the areas under the Ge–Ge and As–As fitted Raman peaks in ratio to the total spectral area.

Our results also reinforce the previous evidence from thermal kinetics that $Ge_{11.5}As_{24}Se_{64.5}$ has the minimum fragility index and thus should be most stable against relaxation.[9] In fact, thermal and optical annealing of Ge–As–Se thin films have confirmed that the refractive index and

the optical bandgap are almost constant under long time thermal annealing or irradiation by subbandgap light,[11,12] whilst our earlier work on film-forming properties suggested that this composition could be evaporated to create films with chemical bonding indistinguishable from the bulk glass.[11] However, the Ge–Ge and As–As bonds are not eliminated for this composition and hence the optical losses would be expected to be significant. Nevertheless, the favorable film-forming properties of this composition make it a good choice for planar waveguides where the interaction pathways are generally short (cm) and hence the intrinsic material losses are generally less important than the fabrication losses associated with factors such as waveguide side-wall roughness. Thus, for waveguide applications, it is more important to have a glass with a stable structure and hence stable optical properties. In fact, the glass with this composition has been successfully used in various optical devices and the stable performance of the devices has been demonstrated.[6,14]

4. Conclusion

We have prepared three groups of Ge–As–Se glasses in which Se is 5.5 mol%, 10 mol%, and 20 mol% rich, respectively. Thermal kinetics analysis of the fragility indicated that the 5.5 mol% Se-rich $Ge_{11.5}As_{24}Se_{64.5}$ glass exhibits the minimum fragility and thus is most stable against structural relaxation. Analysis of the results through decomposing the Raman spectra into different structural units showed that the minimum number of the Ge–Ge and As–As homopolar bonds can be found in $Ge_{15}As_{14}Se_{71}$ glass but these homopolar bonds can never be completely suppressed. The glasses with low fragility, the minimum number of homopolar bonds, and thus lowest optical loss are promising for applications in photonics.

References

[1] Wang R P 2014 *Amorphous Chalcogenides: Advances and Applications* (Singapore: Pan Stanford Publishing) pp. 97–141

[2] Tanaka K and Shimakawa K 2011 *Amorphous Chalcogenide Semiconductors and Related Materials* (New York: Springer International Publishing) pp. 115–123

[3] Wang Z W, Wang X F, Liu C L, Zhao X J, Xiang H, Yu J G, Gong Q H and Gu S X 2005 *Chin. Phys. B* **14** 0551

[4] Qiao B J, Chen F F, Huang Y C, Dai S X, Nie Q H and Xu T F 2015 *Acta Phys. Sin.* **64** 154216 (in Chinese)

[5] Sun J, Nie Q H, Wang G X, Wang X S, Dai S X, Zhang W, Song B A, Shen X and Xu T F 2011 *Acta Phys. Sin.* **60** 114212 (in Chinese)

[6] Eggleton B J, Luther-Davies B and Richardson K 2011 *Nat. Photon.* **5** 141

[7] Zhang Z Y, Chen F, Lu S B, Wang Y H, Shen X, Dai S X and Nie Q H 2015 *Chin. Phys. B* **24** 066801

[8] Wang T, Gai X, Wei W H, Wang R P, Yang Z Y, Shen X, Madden S and Luther-Davies B 2014 *Opt. Mater. Express* **4** 1011

[9] Wang T, Gulbiten O, Wang R P, Yang Z Y, Smith A, Luther-Davies B and Lucas P 2014 *J. Phys. Chem. B* **118** 1436

[10] Wei W H, Wang R P, Shen X, Fang L and Luther-Davies B 2013 *J. Phys. Chem. C* **117** 16571

[11] Bulla D A P, Wang R P, Prasad A, Rode A V, Madden S J and Luther-Davies B 2009 *Appl. Phys. A* **96** 615

[12] Su X Q, Wang R P, Luther-Davies B and Wang L 2013 *Appl. Phys. A* **113** 575

[13] Wang R P, Smith A, Luther-Davies B, Kokkonen H and Jackson I 2009 *J. Appl. Phys.* **105** 056109

[14] Gai X, Han T, Prasad A, Madden S, Choi D Y, Wang R P, Bulla D and Luther-Davies B 2010 *Opt. Express* **18** 26635

[15] Prasad A, Zha C J, Wang R P, Smith A, Madden S and Luther-Davies B 2008 *Opt. Express* **16** 2804

[16] Wang R P, Choi D Y, Rode A V, Madden S J and Luther-Davies B 2007 *J. Appl. Phys.* **101** 113517

[17] Xu S W, Wang R P, Luther-Davies B, Kovalskiy A, Miller A C and Jain H 2014 *J. Appl. Phys.* **115** 083518

[18] Xu S W, Wang R P, Yang Z Y, Wang L and Luther-Davies B 2015 *Appl. Phys. Express* **8** 015504

[19] Popescu M A 2000 *Non-Crystalline Chalcogenides* (Dordrecht: Kluwer Academic Publishers) pp. 55–59

[20] Wang R P, Zha C J, Rode A V, Madden S J and Luther-Davies B 2007 *J. Mater. Sci.: Mater. Electron.* **18** S419

[21] Choi D Y, Madden S, Rode A, Wang R P and Luther-Davies B 2007 *Appl. Phys. Lett.* **91** 011115

[22] Tronc P, Bensoussan M, Brenac A and Sebenne C 1973 *Phys. Rev. B* **8** 5947

[23] Stevens M, Boolchand P and Hernandez J G 1985 *Phys. Rev. B* **31** 981

[24] Kumagai N, Shirafuji J and Inuishi Y 1977 *J. Phys. Soc. Jpn.* **42** 1262

[25] Jackson K, Briley A, Grossman S, Porezag D V and Pederson M R 1999 *Phys. Rev. B* **60** R14985

[26] Yang G, Bureau B, Rouxel T, Gueguen Y, Gulbiten O, Roiland C, Soignard E, Yarger J L, Troles J, Sangleboeuf J C and Lucas P 2010 *Phys. Rev. B* **82** 195206

[27] Li W, Seal S, Rivero C, Lopez C, Richardson K, Pope A, Schulte A, Myneni S, Jain H, Antoine K and Miller A C 2005 *J. Appl. Phys.* **98** 053503

[28] Kohoutek T, Wagner T, Vlcek M, Vlcek M and Frumar M 2006 *J. Non-Cryst. Solids* **352** 1563

[29] Lin F Y, Gulbiten O, Yang Z Y, Calvez L and Lucas P 2011 *J. Phys. D* **44** 045404

[30] Bues W, Somer M and Brockner W 1980 *Z. Naturforsch.* **35b** 1063